minerals

MDPI

Article

Effect of Silica Alumina Ratio and Thermal Treatment of Beta Zeolites on the Adsorption of Toluene from Aqueous Solutions

Elena Sarti [1], Tatiana Chenet [1], Luisa Pasti [1,*], Alberto Cavazzini [1], Elisa Rodeghero [2] and Annalisa Martucci [2]

1 Department of Chemical and Pharmaceutical Sciences, University of Ferrara, Via Fossato di Mortara 17, 44121 Ferrara, Italy; elena.sarti@unife.it (E.S.); tatiana.chenet@unife.it (T.C.); alberto.cavazzini@unife.it (A.C.)

2 Department of Physics and Earth Sciences, University of Ferrara, Via Saragat 1, 44122 Ferrara, Italy; elisa.rodeghero@unife.it (E.R.); annalisa.martucci@unife.it (A.M.)

* Correspondence: luisa.pasti@unife.it; Tel.: +39-0532-455-346

Academic Editor: Huifang Xu

Received: 23 December 2016; Accepted: 10 February 2017; Published: 15 February 2017

Abstract: The adsorption of toluene from aqueous solutions onto hydrophobic zeolites was studied by combining chromatographic, thermal and structural techniques. Three beta zeolites (notated BEAs, since they belong to BEA framework type), with different SiO_2/Al_2O_3 ratios (i.e., 25, 38 and 360), before and after calcination, were tested as adsorbents of toluene from aqueous media. This was performed by measuring the adsorbed quantities of toluene onto zeolites in a wide concentration range of solute. The adsorption data were fitted with isotherms whose models are based on surface heterogeneity of the adsorbent, according to the defective structure of beta zeolites. The thermal treatment considerably increases the adsorption of toluene, in the low concentration range, on all BEAs, probably due to surface and structural modifications induced by calcination. Among the calcined BEAs, the most hydrophobic zeolite (i.e., that with SiO_2/Al_2O_3 ratio of 360) showed the highest binding constant, probably due to its high affinity for an organophilic solute such as toluene. The high sorption capacity was confirmed by thermogravimetric analyses on BEAs, before and after saturation with toluene.

Keywords: adsorption; zeolites; beta; toluene

1. Introduction

In recent years public concern has been rapidly grown regarding water pollution phenomena. Petroleum hydrocarbons represent one of the most common categories of water pollutants. Gasoline leakage from storage tank, transportation, pipelines and petrochemical wastewaters introduce these compounds into the environment, making surface waters and/or groundwaters unsuitable for many uses, including drinking [1]. BTEX (Benzene, toluene, ethylbenzene and xylene) are frequently detected in chemical and petrochemical wastewaters. These contaminants can cause adverse health effects to humans even at low concentrations [2]. Therefore their removal from groundwater and surface waters is a problem of great importance. Among several techniques developed for BTEX removal from waters, adsorption is one of the most efficient methods, thanks to satisfactory efficiencies even at low concentrations [3], easy operation and low cost [4]. Recently, high-silica zeolites have been shown to be environmental friendly materials able to efficiently sorb several organic pollutants from water, such as pharmaceuticals [5–7], polycyclic aromatic hydrocarbons [8], phenols [9] and petrol-derived compounds [10–12].

In literature, several works have focused on the advantages of zeolites as adsorbents, such as high selectivity and capacity, rapid kinetics, reduced interference from salt and humic substances, excellent

resistance to chemical, biological, mechanical and thermal stress [9,13,14]. Even if zeolites are more expensive with respect to other adsorbents, they offer the possibility to be regenerated without loss of performances at relatively low temperatures, as demonstrated in previous works [10,15].

The investigation of several synthetic zeolites such as ZSM-5 [10], mordenite [4], ferrierite [16] and Y [11] for the removal of petrol-derived compounds from aqueous solutions showed that they are a promising material for water clean-up procedures. Another adsorbent that could be employed in such treatment is zeolite beta due to its large porosity and high surface area. Zeolite beta, indeed, has a three-dimensional intersecting channels system, two mutually perpendicular straight channels each with a cross section of 6.6 Å × 6.7 Å and a sinusoidal channel with a cross section of 5.6 Å × 5.6 Å [17]. This tortuous channels system is constituted by the intersection of the two main channels. The channel intersections of zeolite beta generate cavities whose sizes are in the order of 12–13 Å [17]. Crystallographic faults are frequently observed in beta zeolite and a structural model was proposed by Jansen et al. [18] to explain the creation of local defects by the connection of distorted layers. The structure of zeolite beta is disordered along [00l] and it is related to three ordered structures by $a/3$ and/or $b/3$ displacements. The three ordered polytypes are designated frameworks A, B, and C [19,20]. Polytype A is tetragonal (space group $P4_122$ or $P4_322$, cell parameters $a = b \approx 12.5$ Å and $c \approx 26.4$ Å), polytype B is monoclinic (space group $C2/c$, cell parameters $a \approx b \approx 17.6$ Å, $c \approx 14.4$ Å and $\beta \approx 114^\circ$), as well as Polytype C (space group $P2/c$, cell parameters $a \approx b \approx 12.5$ Å, $c \approx 27.6$ Å, and $\beta \approx 107^\circ$).

It has been reported that thermal and hydrothermal treatments induce chemical and structural modifications in beta zeolites, for instance Trombetta et al. [21] observed that thermal treatments can cause dealumination and formation of extraframework aluminium species. The ease of dealumination of beta may be due to the presence of defect sites close to the framework aluminium which promotes bond hydrolysis, nonetheless the microporous structure is not affected by the loss of aluminium [22]. Other zeolites, such as ZSM-5 or mordenite, do not show significant crystallinity loss or dealumination after thermal treatment [10,15,22]. The precise structural modifications of beta zeolite are still a matter of research and the global effect of calcination on beta acidity is not totally clear, because of the presence of several types of acidic sites, with different acidity degree [23,24]. However, it can be inferred that beta zeolites could undergo to greater variations in adsorption properties due to calcination with respect to other zeolites. Also the hydrophilic/hydrophobic features, controlled by varying the SiO_2/Al_2O_3 ratio (SAR), can influence the behaviour of zeolites towards polar/non-polar reactants and products in adsorption and catalytic processes. In fact, the roles played both by calcination and by SAR on catalytic activity of beta zeolites received great attention [25,26]. However there are only few works dealing with the effects of both chemical the composition and thermal treatments of beta on the adsorption properties toward solutes from water solutions. Indeed, the phenomena observed in catalytic gas phase systems could be different from those in aqueous matrix, since it has already been reported that the presence of water can strongly interfere with organic compounds adsorption [27].

Therefore, the objective of this work is to investigate the adsorptive properties of beta zeolites (notated BEAs, since they belong to BEA framework type), with different Silica/Alumina ratios (SAR) before and after calcination for the removal of toluene (TOL) from aqueous solutions. The selected adsorbents were commercial beta zeolites: the possibility to find them on the market and to use them as-received from the manufacturer was considered a strong decision point for their selection.

2. Materials and Methods

2.1. Chemicals

Toluene (99% purity) was obtained from Sigma-Aldrich (Steinheim, Germany). High-performance liquid chromatography (HPLC) grade acetonitrile (ACN) was purchased from Merck (Darmstadt, Germany). The water was Milli-Q grade (Millipore, Billerica, MA, USA). Zeolite beta powders were obtained from Zeolyst International (Conshohocken, PA, USA) and their main characteristics are reported in Table 1.

Table 1. Zeolites characteristics.

Name	Product Code	SiO_2/Al_2O_3	Nominal Cation	Surface Area ($m^2 \cdot g^{-1}$)
Beta25	CP814E	25	Ammonium	680
Beta38	CP814C	38	Ammonium	710
Beta360	CP811C-300	360	Hydrogen	620

All the adsorbents were employed as-received (named Beta25, Beta38 and Beta360) and after a calcination process (referred to as Beta25c, Beta38c and Beta360c). Calcination was carried out by raising the temperature from room temperature to 600 °C in 1 h, then holding at 600 °C for 4 h. Finally, adsorbents were kept at room temperature for 3 h. Dry air circulation was maintained during both heating and cooling down. The calcined samples were kept in a desiccator and used within 2 days after thermal treatment.

2.2. Experimental

The adsorption isotherm was determined using the batch method. Batch experiments were carried out in duplicate in 20 mL crimp top reaction glass flasks sealed with polytetrafluoroethylene (PTFE) septa (Supelco, Bellefonte, PA, USA). The flasks were filled in order to have the minimum headspace and a solid/solution ratio of 1:2 ($mg \cdot mL^{-1}$) was employed. After equilibration, for 24 h at a temperature of 25.3 ± 0.5 °C under stirring, the solids were separated from the aqueous solution by filtration trough 0.22 μm polyvinylidene fluoride (PVDF) membrane filters purchased from Agilent Technologies (Santa Clara, CA, USA). The concentration of TOL was determined in the solutions before and after equilibration with zeolite by High Performance Liquid Chromatography/Diode Array Detection (HPLC/DAD) purchased from Waters (Waters Corporation, Milford, MA, USA).

2.3. Instrumentation

The HPLC/DAD was employed under isocratric elution conditions. The column (Agilent Technologies) was 150 mm × 4.6 mm, packed with a C18 silica-based stationary phase with a particle diameter of 5 μm and thermostated at 25 °C. The injection volume was 20 μL for all standards and samples. The mobile phase was a mixture ACN:H_2O 70:30 and the flow rate was 1 mL/min. Detection wavelength was set at 215 nm Thermogravimetric (TG), differential thermogravimetric (DTG) and differential thermal analyses (DTA) measurements of exhausted samples were performed in air up to 900 °C, at 10 $°C \cdot min^{-1}$ heating rate, using a simultaneous thermal analysis (STA) 409 PC LUXX®—NETZSCH Gerätebau GmbH (Verona, Italy). X-ray powder diffraction (XRPD) patterns of zeolites after TOL adsorption were measured on a Bruker (Billerica, MA, USA) D8 Advance Diffractometer equipped with a Si (Li)SOL-X solid-state detector. Statistical elaborations were carried out through MATLAB® ver. 9.1 software (The MathWorks Inc., Natick, MA, USA).

3. Results and Discussion

3.1. Adsorption from Aqueous Solutions

The adsorption kinetics was studied in order to obtain some important parameters, such as the kinetic constant, which allow the estimation of the time requested for reaching the equilibrium. Moreover, from kinetics measurements, qualitative information about the steps governing the adsorption process can be gained. The uptake q ($mg \cdot g^{-1}$) was calculated as follows:

$$q = \frac{(C_0 - C_e)V}{m} \quad (1)$$

where C_0 is the initial concentrations in solution ($mg \cdot L^{-1}$), C_e is the concentration at time t in kinetics experiments or at equilibrium ($mg \cdot L^{-1}$) for isotherm modelling, V is the solution volume (L) and m is the mass of adsorbent (g).

The kinetics was very fast for all the studied materials and the time to reach equilibrium was about 10 min. As an example, the uptake data obtained for TOL on Beta360 are shown in Figure 1. The data of Figure 1 were fitted by the pseudo-second order model (Equation (2)), which has been employed in many studies concerning the adsorption of organic compounds onto zeolites [28,29].

$$q_t = \frac{k_2 q^2 t}{1 + k_2 q t} \tag{2}$$

where q_t and q are the amounts of solute sorbed per mass of adsorbent at time t and at equilibrium, respectively, and k_2 is the second-order adsorption rate constant. The equilibrium uptake q and the adsorption rate constant k_2 were obtained from non-linear fit of q_t vs. t. Values of 3.39 (3.28, 3.50) and 0.46 (0.31, 0.62) were obtained for q_e and k_2, respectively: the confidence limits at 95% of probability are reported in brackets. The pseudo-second-order model fitted well all the sorption data as demonstrated by the resulting high coefficients of determination (R^2 = 0.9915). From Figure 1 it can also be seen that the surface adsorption (first part of the curve) is a faster process than the intraparticle diffusion of TOL into the zeolite micropores as alredy observed for ZSM-5 [10].

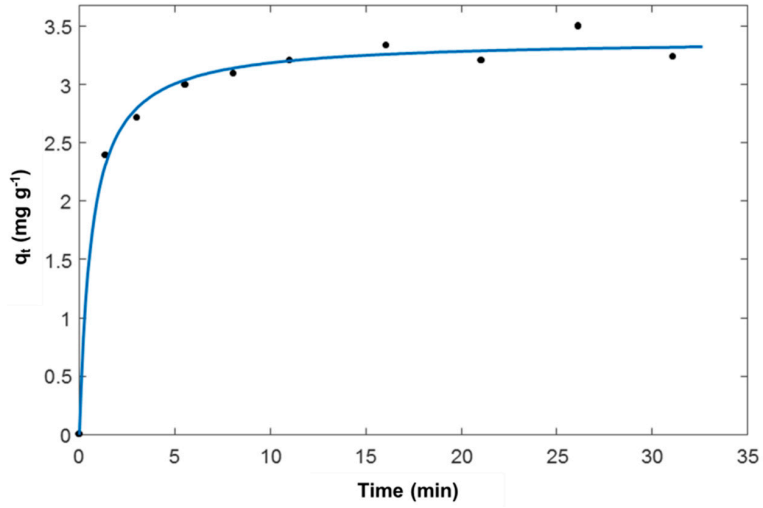

Figure 1. Adsorption kinetics of toluene (TOL) on Beta360: TOL uptake vs. contact time.

The relationship between the solute amount adsorbed for per unit mass of adsorbent q and its concentration at equilibrium C_e is provided by equilibrium adsorption isotherms. The Langmuir isotherm has been frequently used to describe the adsorption of organics in aqueous solutions onto hydrophobic zeolites [10,15,29]. This model considers a monolayer adsorption onto energetically equivalent adsorption sites and negligible sorbate–sorbate interactions. It can be represented by the following equation [30].

$$q = \frac{q_S b C_e}{1 + b C_e} \tag{3}$$

where b is the binding constant (L·mg^{-1}) and q_s is the saturation capacity of the adsorbent material (mg·g^{-1}). This model has already been employed for adsorption on BEAs of several classes of organic compounds, such as pharmaceuticals [6], etheramine [29], xylene isomers and ethylbenzene [31].

Freundlich isotherm is a relationship describing non-ideal and reversible adsorption, not restricted to the formation of monolayer. In fact, this empirical model can be applied to multilayer adsorption, with non-uniform distribution of adsorption heat and affinities over the heterogeneous surface [32]. The Freundlich isotherm model can be expressed as [33].

$$q = K_F {C_e}^{1/n} \tag{4}$$

where K_F is a constant indicative of the adsorption capacity and $1/n$ is a measure of the surface heterogeneity, ranging between 0 and 1. The surface heterogeneity increases as $1/n$ gets closer to zero. The Freundlich isotherm equation was found to have a better fit than the Langmuir equation for TOL adsorption on as-received BEAs (vide infra). This model was also used also by Wang et al. [28] for describing the adsorption of 1,3-propanediol on BEAs zeolites.

Another isotherm model employed to describe multiple adsorbate/adsorbent interactions is that proposed by Tóth [34].

$$q = \frac{q_S b C_e}{[1 + (bC_e)^v]^{1/v}} \quad (5)$$

where v is a parameter accounting for the heterogeneity of adsorption energies. If v = 1, the Tóth model corresponds to the Langmuir model [34].

The adsorption isotherms of TOL on both as-received and calcined BEAs are shown in Figure 2, where it can be noted that the isotherms shape of as-received and calcined beta zeolites are different from each other mainly due to modification on the adsorbate/surface interaction energy caused by calcination of the adsorbent. In particular, the thermal treatment considerably increases the adsorption efficiency of all BEAs toward TOL in the low concentration range. This finding has also been observed also for polar compounds such as pharmaceuticals [6]. It has been suggested that part of the adsorption properties of BEA zeolites originates from faults in the zeolitic structure [35]. In addition to its Brønsted acidity, beta zeolite also displays also Lewis acidity [36]. The calcination leads to the conversion of NH_4-BEA to H-BEA for Beta25 and Beta38 (see Table 1), as well as to structural and surface modifications for all the three beta zeolites [36,37]. In particular, the thermal treatment can lead to silanols condensation and, consequently, to the degradation of Brønsted acid sites by dehydroxylation. Together with the removal of water, the formation of Lewis acid sites occurs [24], as proposed by some studies [21,23] which found an increase in the ratio Lewis/Brønsted acid sites in the calcined material with respect to the as-received one. However, the global effect of calcination on beta acidity is not totally clear, because of the presence of several types of acidic sites, with different acidity degree [24,38]. It can be inferred that beta Lewis acid sites, whose formation has been promoted by thermal treatment, could interact with toluene as reported by Maretto et al. [39]. Therefore, calcination can lead to structural and compositional changes in beta zeolites, inducing to differences in adsorption properties [22,40]. The experimental data were fitted with all the three models (see Equations (3)–(5)). In order to compare these models, the statistical analysis of the fitting based of the square sum of errors and the number of parameters was performed. The isotherm parameters of the best fitted model estimated by non-linear fitting of the as-received and calcined BEAs are shown in Tables 2 and 3, respectively.

Table 2. Isotherm parameters for the adsorption of TOL on as-received BEAs estimated by non-linear fitting, according to the Freundlich model. The confidence limits at 95% of probability of the estimated parameters are reported in brackets.

As-Received Materials	K_F (mg·g^{-1})·(L·g^{-1})^n	n	R^2
Beta25	5.2 (3.5, 7.0)	0.86 (0.77, 0.95)	0.9953
Beta38	4.2 (2.5, 5.9)	0.79 (0.69, 0.89)	0.9936
Beta360	4.1 (2.8, 5.3)	0.93 (0.72, 1.1)	0.9956

Table 3. Isotherm parameters for the adsorption of TOL on calcined BEAs estimated by non-linear fitting, according to the Tóth model. The confidence limits at 95% of probability of the estimated parameters are reported in brackets.

Calcined Materials	q_s (mg·g^{-1})	b (L·mg^{-1})	v	R^2
Beta25c	234 (193, 275)	0.073 (0.043, 0.10)	0.96 (0.70, 1.2)	0.9584
Beta38c	224 (198, 250)	0.10 (0.075, 0.13)	0.91 (0.72, 1.1)	0.9688
Beta360c	241 (201, 280)	0.55 (0.30, 0.80)	0.84 (0.62, 1.0)	0.9667

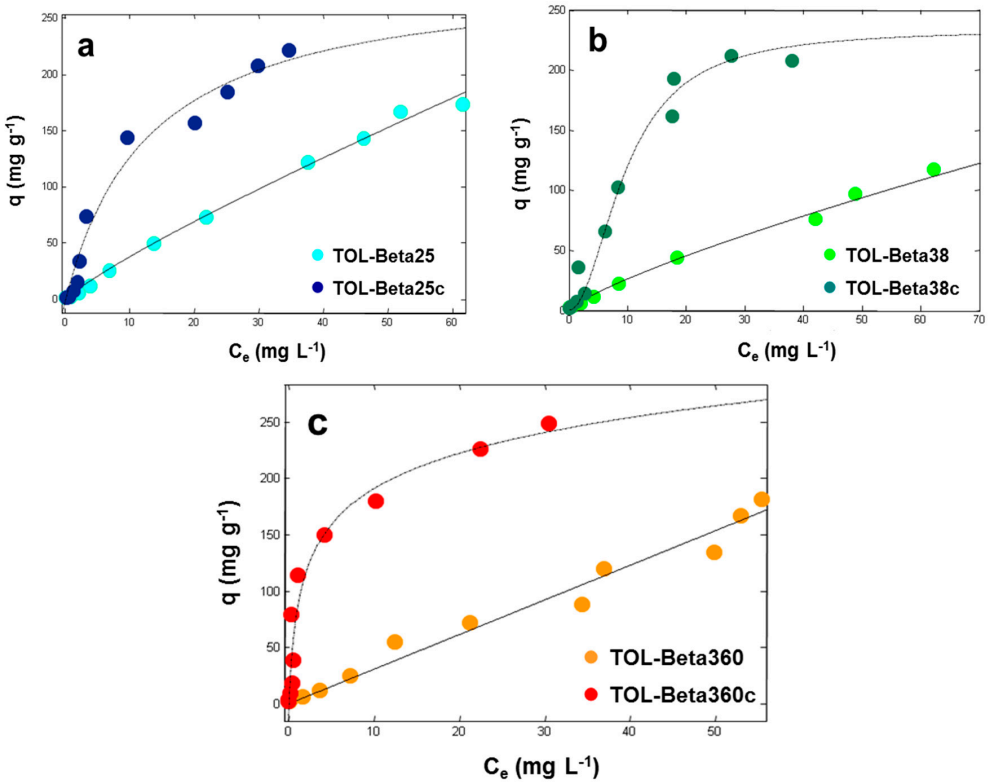

Figure 2. Adsorption isotherms of TOL on (**a**) Beta25 (light blue circles: as-received, dark blue circles: calcined); (**b**) Beta38 (light green circles: as-received, dark green circles: calcined) and (**c**) Beta360 (orange circles: as-received, red circles: calcined).

From Tables 2 and 3, it can be seen that as-received zeolites are fitted well by a Freundlich model, whereas the calcined materials are modelized by a Tóth isotherm equation. In particular, Table 2 shows that n constant for Beta360 is not statistically different, at 95% of probability, from 1, hence TOL adsorption on this zeolite follows a linear trend. On the contrary, values of n below 1 have been observed for both Beta25 and Beta38, indicating that the adsorbent surface is heterogeneous. The values of K_F found for the three as-received BEAs are not statistically different from each other at a probability of 95%. This finding may indicate similar adsorbent/adsorbate interactions, possibly due to the effect of physisorbed water on the zeolites porosities (see Section 3.2) and to the presence of structural defects in beta zeolites that make it difficult to assess the properties of the adsorption sites. By comparing calcined BEAs (Table 3), it can be seen that their saturation capacities are not statistically different at 95% of probability. High values of q_s were obtained for all the calcined adsorbents (above 20% w/w). This last finding makes calcined BEAs very promising as adsorbents in the remediation of contaminated waters at high concentration levels. Similar values of q_s were found in the adsorption of different organic contaminants on hydrophobic Y zeolite (FAU-type framework topology) [11,12]. However, the binding constants b obtained with Y zeolite were quite low, thus indicating that in the low concentrations range Y zeolite is generally less efficient than calcined BEAs. At low TOL concentrations, it has been proved that another hydrophobic zeolite, namely ZSM-5 (MFI-type framework topology) is very efficient [10]. In this case, in fact, the adsorption isotherm of TOL on ZSM-5 was characterized by a high binding constant (b was 3.17 $\pm$ 0.41), despite the lower saturation capacity of ZSM-5 than BEAs and Y (around 8% w/w). In the light of the above findings, it can be stated that calcined BEAs represent a good compromise for that which concerning TOL adsorption from aqueous solutions in a wide concentrations range. Concerning the binding constant b, Beta360c showed a higher value than those of Beta25c and Beta38c, which are not significantly different from each other at 95% of probability. This finding could be explained by considering that adsorption onto zeolites is driven by

both electrostatic and non-covalent interactions [41]. It can be supposed that electrostatic interactions have a negligible contribution to the adsorption of an organophilic solute such as TOL, characterized by $\log K_{ow}$ of 2.73. Therefore, it can be considered that the adsorption mechanism of TOL onto BEAs is driven mainly by non-covalent interactions, which become more relevant as SAR value increases.

3.2. Thermal and Structural Analyses

Thermogravimetric analysis were carried out for the as-received materials (i.e., Beta25, Beta38 and Beta360). A total weight loss of about 17% was observed for all the three samples for temperature up to 900 °C.

These weight losses can be divided up into two contributions: the first one at low temperature (i.e., lower than about 100 °C) due to the loss of water molecules weakly bonded to the zeolite surface and the second one at higher temperature mainly ascribable to the loss of ammonia from Beta25 and Beta38 as well as losses of structural water molecules and silanols condendation in all the beta samples (Figure 3).

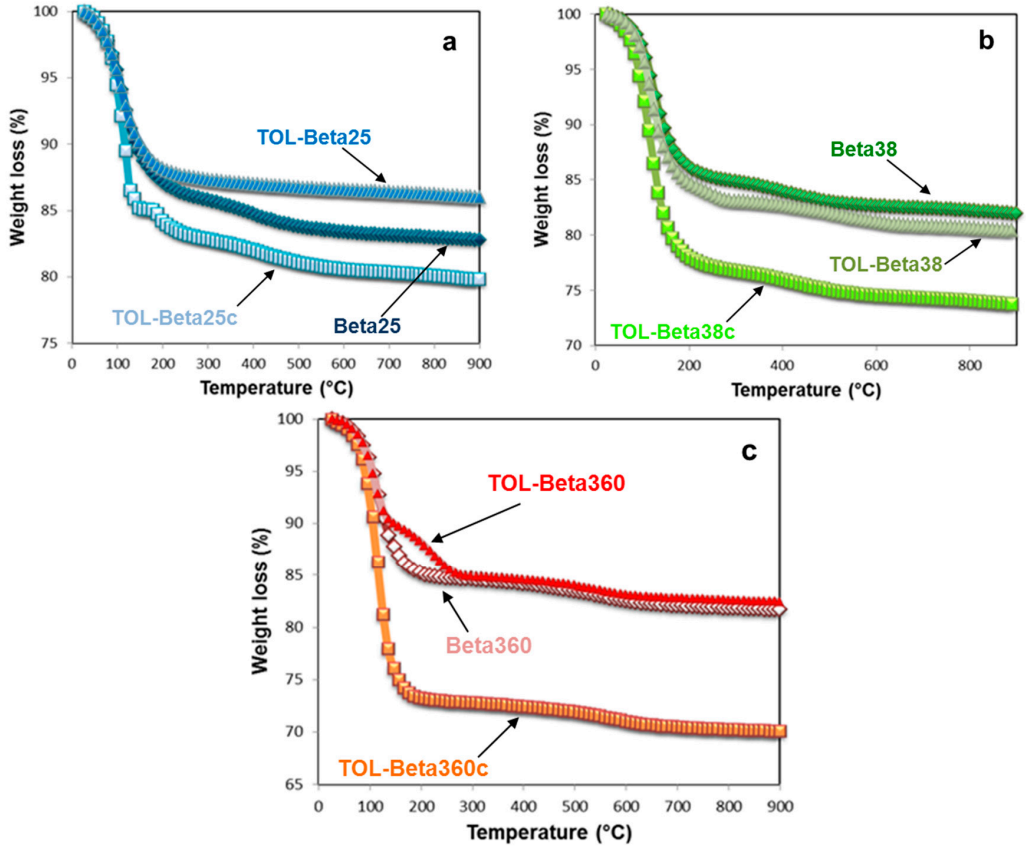

Figure 3. Thermogravimetric curves of as-received and calcined BEAs, before and after saturation with TOL: (**a**) Beta25; (**b**) Beta38; and (**c**) Beta360.

The TG analyses of calcined BEAs after TOL saturation show weight losses at 900 °C of 20.2%, 26.2% and 30% for Beta25c, Beta38c and Beta360c, respectively. However, these weight losses cannot be easly related to the adsorbed TOL amount since, as reported in Pasti et al. [6], the calcined zeolites can undergo to rehydratation process and the temperatures at which the adsorbed water and TOL are removed from the framework are very close to each other's. This makes it difficult to ascribe the whole weight loss to water or TOL alone. However, these results are in good agreement with the saturation capacities of the materials determined by adsorpion experiments (see Table 3).The X-ray powder diffraction patterns of both as-received and calcined Beta25, Beta38 and Beta360, before and

after saturation with TOL are reported in Figure 4. By comparing the X-ray powder diffraction pattern of both the as-received and the calcined materials before and after TOL adsorption (see Figure 4) it can be observed that the peaks intensities in the low 2θ region change thus confirming the incorporation of molecules in the framework due to adsorption, moreover the differences in the patterns in the intermediate and high 2θ region indicates that the process is associated with the framework flexibility (expansion or contraction of the cell volume) [42,43]. Similar behaviour is also shown when the three zeolite samples before and after thermal treatment are compared.

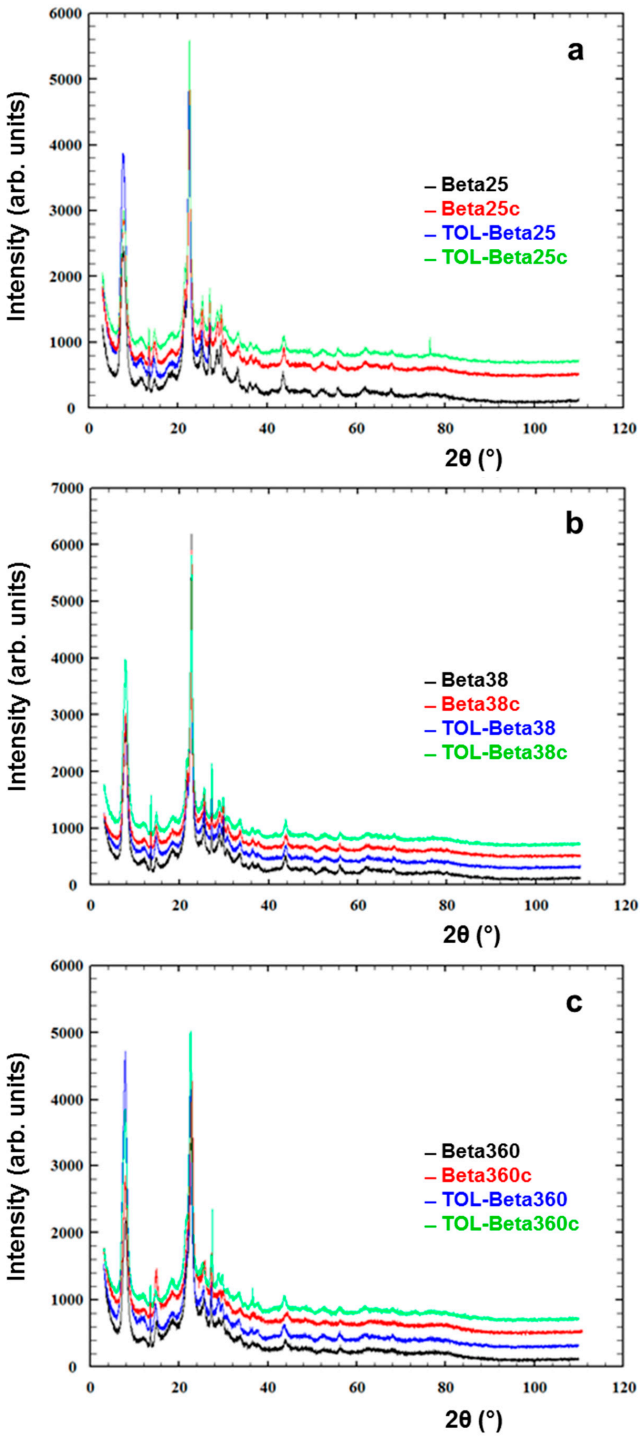

Figure 4. X-ray powder diffraction patterns of as-received and calcined BEAs before and after saturation with TOL: (**a**) Beta25; (**b**) Beta38; and (**c**) Beta360.

4. Conclusions

This work highlighted the differences in adsorption properties between as-received and calcined beta zeolites, with three different SARs, toward a water contaminant of great concern such as toluene. It has been observed that the calcination significantly improves the adsorption properties of all of the three zeolites.

The adsorption of toluene by calcined BEAs is characterized by high values of saturation capacity. The most hydrophobic calcined beta, i.e., Beta360c, showed the highest binding constant, thus indicating stronger adsorbent/adsorbate interactions than those of Beta25c and Beta38c. Consequently, Beta360 after thermal treatment is a promising adsorbent for the removal of toluene in water-containing systems. These results open new alternatives for the industrial application of this material, mainly in hydrocarbons adsorption processes in the presence of water.

Acknowledgments: Federico Giacometti is acknowledged for performing some of the experiments.

Author Contributions: Elena Sarti wrote the paper and performed some of the adsorption experiments with Tatiana Chenet; Luisa Pasti, Alberto Cavazzini and Annalisa Martucci conceived and designed the experiments and analyzed the data; Elisa Rodeghero performed thermogravimetric and X-ray data analysis.

Conflicts of Interest: The authors declare no conflicts of interest.

References

1. Aivalioti, M.; Vamvasakis, I.; Gidarakos, E. BTEX and MTBE adsorption onto raw and thermally modified diatomite. *J. Hazard. Mater.* **2010**, *178*, 136–143. [CrossRef] [PubMed]
2. Qu, F.; Zhu, L.; Yang, K. Adsorption behaviors of volatile organic compounds (VOCs) on porous clay heterostructures (PCH). *J. Hazard. Mater.* **2009**, *170*, 7–12. [CrossRef] [PubMed]
3. Gupta, V.K.; Verma, N. Removal of volatile organic compounds by cryogenic condensation followed by adsorption. *Chem. Eng. Sci.* **2002**, *57*, 2679–2696. [CrossRef]
4. Arletti, R.; Martucci, A.; Alberti, A.; Pasti, L.; Nassi, M.; Bagatin, R. Location of MTBE and toluene in the channel system of the zeolite mordenite: Adsorption and host–guest interactions. *J. Solid State Chem.* **2012**, *194*, 135–142. [CrossRef]
5. Martucci, A.; Pasti, L.; Marchetti, N.; Cavazzini, A.; Dondi, F.; Alberti, A. Adsorption of pharmaceuticals from aqueous solutions on synthetic zeolites. *Microporous Mesoporous Mater.* **2012**, *148*, 174–183. [CrossRef]
6. Pasti, L.; Sarti, E.; Cavazzini, A.; Marchetti, N.; Dondi, F.; Martucci, A. Factors affecting drug adsorption on beta zeolites. *J. Sep. Sci.* **2013**, *36*, 1604–1611. [CrossRef] [PubMed]
7. Braschi, I.; Blasioli, S.; Gigli, L.; Gessa, C.E.; Alberti, A.; Martucci, A. Removal of sulfonamide antibiotics from water: Evidence of adsorption into an organophilic zeolite Y by its structural modifications. *J. Hazard. Mater.* **2010**, *17*, 218–225. [CrossRef] [PubMed]
8. Costa, A.A.; Wilson, W.B.; Wang, H.; Campiglia, A.D.; Dias, J.A.; Dias, S.C.L. Comparison of BEA, USY and ZSM-5 for the quantitative extraction of polycyclic aromatic hydrocarbons from water samples. *Microporous Mesoporous Mater.* **2012**, *149*, 186–192. [CrossRef]
9. Khalid, M.; Joly, G.; Renaud, A.; Magnoux, P. Removal of phenol from water by adsorption using zeolites. *Ind. Eng. Chem. Res.* **2004**, *43*, 5275–5280. [CrossRef]
10. Rodeghero, E.; Martucci, A.; Cruciani, G.; Bagatin, R.; Sarti, E.; Bosi, V.; Pasti, L. Kinetics and dynamic behaviour of toluene desorption from ZSM-5 using in situ high-temperature synchrotron powder X-ray diffractionand chromatographic techniques. *Catal. Today* **2016**, *227*, 118–125. [CrossRef]
11. Martucci, A.; Braschi, I.; Bisio, C.; Sarti, E.; Rodeghero, E.; Bagatin, R.; Pasti, L. Influence of water on the retention of methyl tertiary-butyl ether by high silica ZSM-5 and Y zeolites: A multidisciplinary study on the adsorption from liquid and gas phase. *RSC Adv.* **2015**, *5*, 86997–87006. [CrossRef]
12. Pasti, L.; Martucci, A.; Nassi, M.; Cavazzini, A.; Alberti, A.; Bagatin, R. The role of water in DCE adsorption from aqueous solutions onto hydrophobic zeolites. *Microporous Mesoporous Mater.* **2012**, *160*, 182–193. [CrossRef]
13. Weitkamp, J. Zeolites and catalysis. *Solid State Ion.* **2000**, *131*, 175–188. [CrossRef]

14. Aivalioti, M.; Pothoulaki, D.; Papoulias, P.; Gidarakos, E. Removal of BTEX, MTBE and TAME from aqueous solutions by adsorption onto raw and thermally treated lignite. *J. Hazard. Mater.* **2012**, *207*, 136–146. [CrossRef] [PubMed]
15. Martucci, A.; Rodeghero, E.; Pasti, L.; Bosi, V.; Cruciani, G. Adsorption of 1,2-dichloroethane on ZSM-5 and desorption dynamics by in situ synchrotron powder X-ray diffraction. *Microporous Mesoporous Mater.* **2015**, *215*, 175–182. [CrossRef]
16. Martucci, A.; Leardini, L.; Nassi, M.; Sarti, E.; Bagatin, R.; Pasti, L. Removal of emerging organic contaminants from aqueous systems: Adsorption and location of methyl-tertiary-butylether on synthetic ferrierite. *Mineral. Mag.* **2014**, *78*, 1161–1175. [CrossRef]
17. Baerlocher, C.; Meir, W.M.; Olson, O.H. *Atlas of Zeolite Framework Types*, 5th revised ed.; Elsevier Science: Amsterdam, The Netherlands, 2001.
18. Jansen, J.C.; Creyghton, E.J.; Njo, S.L.; van Koningsveld, H.; van Bekkum, H. On the remarkable behaviour of zeolite Beta in acid catalysis. *Catal. Today* **1997**, *38*, 205–212. [CrossRef]
19. Higgins, J.B.; LaPierre, R.B.; Schlenker, J.L.; Rohrman, A.C.; Wood, J.D.; Kerr, G.T.; Rohrbaugh, W.J. The framework topology of zeolite beta. *Zeolites* **1988**, *8*, 446–452. [CrossRef]
20. Newsam, J.M.; Treacy, M.M.J.; Koetsier, W.T.; De Gruyter, C.B. Structural characterization of zeolite beta. *Proc. R. Soc. Lond. Ser. A* **1988**, *420*, 375–405. [CrossRef]
21. Trombetta, M.; Busca, G.; Storaro, L.; Lenarda, M.; Casagrande, M.; Zambon, A. Surface acidity modifications induced by thermal treatments and acid leaching on microcrystalline H-BEA zeolite. A FTIR, XRD and MAS-NMR study. *Phys. Chem. Chem. Phys.* **2000**, *2*, 3529–3537. [CrossRef]
22. Beyer, H.K.; Nagy, J.B.; Karge, H.G.; Kiricsi, I. *Catalysis by Microporous Materials*; Elsevier: Amsterdam, The Netherlands, 1995.
23. Otomo, R.; Yokoi, T.; Kondo, J.N.; Tatsumi, T. Dealuminated Beta zeolite as effective bifunctional catalyst for direct transformation of glucose to 5-hydroxymethylfurfural. *Appl. Catal. A Gen.* **2014**, *470*, 318–326. [CrossRef]
24. Čejka, J.; van Bekkum, H.; Corma, A.; Schüth, F. *Introduction to Zeolite Science and Practice*, 3rd revised ed.; Elsevier: Amsterdam, The Netherlands, 2007.
25. Al-Khattaf, S.; Ali, S.A.; Aitani, A.M.; Žilková, N.; Kubička, D.; Čejka, J. Recent advances in reactions of alkylbenzenes over novel zeolites: The effects of zeolite structure and morphology. *Catal. Rev.* **2014**, *56*, 333–402. [CrossRef]
26. Dědeček, J.; Sobalík, Z.; Wichterlová, B. Siting and distribution of framework aluminium atoms in silicon-rich zeolites and impact on catalysis. *Catal. Rev.* **2012**, *54*, 135–223. [CrossRef]
27. Krishna, R.; van Baten, J.M. Hydrogen bonding effects in adsorption of water–alcohol mixtures in zeolites and the consequences for the characteristics of the Maxwell–Stefan diffusivities. *Langmuir* **2010**, *26*, 10854–10867. [CrossRef] [PubMed]
28. Wang, Z.; Wu, Z.; Tan, T. Sorption equilibrium, mechanism and thermodynamics studies of 1,3-propanediol on beta zeolite from an aqueous solution. *Bioresour. Technol.* **2013**, *145*, 37–42. [CrossRef] [PubMed]
29. Magriotis, Z.M.; Leal, P.V.B.; de Sales, P.F.; Papini, R.M.; Viana, P.R.M.; Augusto Arroyo, P. A comparative study for the removal of mining wastewater by kaolinite, activated carbon and beta zeolite. *Appl. Clay Sci.* **2014**, *91*, 55–62. [CrossRef]
30. Langmuir, I. The adsorption of gases on plane surfaces of glass, mica and platinum. *J. Am. Chem. Soc.* **1918**, *40*, 1361–1403. [CrossRef]
31. Dehkordi, A.M.; Khademi, M. Adsorption of xylene isomers on Na-BETA zeolite: Equilibrium in batch adsorber. *Microporous Mesoporous Mater.* **2013**, *172*, 136–140. [CrossRef]
32. Foo, K.Y.; Hameed, B.H. Insights into the modeling of adsorption isotherm systems. *Chem. Eng. J.* **2010**, *156*, 2–10. [CrossRef]
33. Freundlich, H.M.F. Over the adsorption in solution. *J. Phys. Chem.* **1906**, *57*, 385–471.
34. Tóth, J. State equations of the solid gas interface layer. *Acta Chem. Acad. Sci. Hung.* **1971**, *69*, 311–317.
35. Camblor, M.A.; Pérez-Pariente, J. Crystallization of zeolite beta: Effect of Na and K ions. *Zeolites* **1991**, *11*, 202–210. [CrossRef]
36. Kunkeler, P.J.; Zuurdeeg, B.J.; van der Waal, J.C.; van Bokhoven, J.A.; Koningsberger, D.C.; van Bekkum, H. Zeolite Beta: The relationship between calcination procedure, aluminum configuration, and lewis acidity. *J. Catal.* **1998**, *180*, 234–244. [CrossRef]

37. Lohse, U.; Altrichter, B.; Fricke, R.; Pilz, W.; Schreier, E.; Garkisch, C.; Jancke, K. Synthesis of zeolite beta Part 2—Formation of zeolite beta and titanium-beta via an intermediate layer structure. *J. Chem. Soc. Faraday Trans.* **1997**, *93*, 505–512. [CrossRef]
38. Kiricsi, I.; Flego, C.; Pazzuconi, G.; Parker, W.O.; Millini, R.; Perego, C.; Bellussi, G. Progress toward understanding zeolite β acidity: An IR and ^{27}Al NMR spectroscopic study. *J. Phys. Chem.* **1994**, *98*, 4627–4634. [CrossRef]
39. Maretto, M.; Vignola, R.; Williams, C.D.; Bagatin, R.; Latini, A.; Petrangeli Papini, M. Adsorption of hydrocarbons from industrial wastewater onto a silica mesoporous material: Structural and thermal study. *Microporous Mesoporous Mater.* **2015**, *203*, 139–150. [CrossRef]
40. Burke, N.R.; Trimm, D.L.; Howe, R.F. The effect of silica:alumina ratio and hydrothermal ageing on the adsorption characteristics of BEA zeolites for cold start emission control. *Appl. Catal. B Environ.* **2003**, *46*, 97–104. [CrossRef]
41. Krohn, J.E.; Tsapatsis, M. Amino acid adsorption on zeolite β. *Langmuir* **2005**, *21*, 8743–8750. [CrossRef] [PubMed]
42. Sánchez-Gil, V.; Noya, E.G.; Sanz, A.; Khatib, S.J.; Guil, J.M.; Lomba, E.; Marguta, R.; Valencia, S. Experimental and simulation studies of the stepped adsorption of toluene on pure-silica MEL zeolite. *J. Phys. Chem. C* **2016**, *120*, 8640–8652. [CrossRef]
43. Dong, J.; Tian, T.; Ren, L.; Zhang, Y.; Xu, J.; Cheng, X. CuO nanoparticles incorporated in hierarchical MFI zeolite as highlyactive electrocatalyst for non-enzymatic glucose sensing. *Colloid Surf. B* **2015**, *125*, 206–212. [CrossRef] [PubMed]